Journal of Magnetism and Magnetic Materials 515 (2020) 167297

Contents lists available at ScienceDirect

Journal of Magnetism and Magnetic Materials

journal homepage: www.elsevier.com/locate/jmmm

Giant magnetoreactance in magnetic nanowires

Andrzej Janutka*, Kacper Brzuszek

Department of Theoretical Physics, Wroclaw University of Science and Technology, 50-370 Wrocław, Poland

ARTICLE INFO

Keywords:
Ferromagnetic nanowire
Micromagnetic simulations
Dynamics of domain structures
Giant magnetoreactance

ABSTRACT

We outline the idea of magnetic-field sensing with a nanometer spatial resolution using the effect of giant magnetoreactance (GMX) and we discuss results of our micromagnetic studies of domain-wall-assisted (or double-vortex-assisted) GMX in nanomagnets. By analogy to low-frequency giant magnetoimpedance (GMI), we consider systems of domains magnetized perpendicular to the direction of the AC current that creates an alternating Oersted field, thus, it drives the DW oscillations. Because of small cross-sections, the nanomagnets are not capable to induce large changes of the magnetic flux, therefore, the impedance of magnet-containing nanocircuits is dominated by the static resistivity (in accessible frequency regimes), while, GMX is an alternative effect to be utilized for sensing. We analyze in detail the effect in single-crystalline nanowire of cobalt with the easy axis transverse to the nanowire axis. In that system, small coherent shifts of the domain walls (DWs) induce relatively high changes of the magnetic flux through the largest cross-section of the nanowire due to large density of periodically packed DWs. Driven by the alternating transverse field of the Oersted origin, the system allows for perpendicular (the field directed perpendicular to the long axis of the nanowire and to the domain magnetization) GMX of improved characteristics (the GMX ratio and the field sensitivity of GMX) at a high stability of the magnetic structure in a wide region of the external field. Moreover, due to a non-zero overall magnetization (created by DWs), the perpendicular GMX is strongly asymmetric with respect to the field reversal (in a low-field regime). Also, we study the transverse GMX (the field parallel to the domain magnetization).

1. Introduction

The giant-magnetoimpedance (GMI) effect in microwires and multilayered microstructers is studied for above two decades with relevance to sensing magnetic fields with a very high field-sensitivity [1–4]. The spatial resolution of the GMI sensors is limited by the sizes of the ferromagnets used, which raises the question about the capabilities of the ultimate miniaturization of magnet-containing inductive circuits. The dominant mechanisms of GMI, skin effect in microwires and coherent magnetization rotation in magnetic multilayers, become irrelevant at the nanoscale. In the accessible (GHz) range of the AC frequency, the skin effect is absent since the skin depth overcomes the diameters of the magnet cross-sections [5], while, the coherent rotation of the domain magnetization beyond the ferromagnetic resonance (FMR) is suppressed by the magnetostatics (a large surface-to-volume ratio) [6]. Moreover, small cross-sections of the magnetic nanosystems are not capable to carry a large magnetic flux. Therefore, except for layered systems at the FMR frequencies [5,7], the inductive contribution to the impedance is weak compared to the static resistance [8]. For that case, an alternative to sensing with the magnetoimpedance (MI) is utilizing the magnetoreactance (MX) which can be a giant effect even in the absence of GMI [9–12].

With regard to miniaturizing sensors, previously, the authors have discussed MX in three different ferromagnetic nanosystems: a nanotube, a nanostripe, and a layered nanomagnet of the H-letter shape [13–15]. Note that in [13,14], the name GMI has been confusingly used instead of GMX, (the reactance is the imaginary part of the impedance, however, the correct usage of the term MI relates to the field dependence of the impedance modulus). In the later system (the H-shaped nanomagnet, Fig. 1a), impedant effects follow from the oscillatory motion of a double-vortex (the oscillations of the distance between vortices), which is driven by the alternating Oersted field. In the former two: the nanotube and the nanostripe, the giant magnetoreactance (GMX) follows from the oscillatory motion of domain walls which are aligned transversely to the long axis of the magnet. The motion along the nanowire induces the electromotive force in an inductive loop of Fig. 1b,c. The mechanism first studied by Valenzuela with relevance to low-frequency regime of MI (below the frequency of the skin-effect appearance [16,17]) is valid to magnetic nanosystems in the GHz range of the driving-current frequency. Note that the DW motion in micrometer-sized systems affects GMI also in the intermediate-frequency regime via modifying the skin depth of the microwires or amplitude of the

* Corresponding author.
E-mail address: Andrzej.Janutka@pwr.edu.pl (A. Janutka).

https://doi.org/10.1016/j.jmmm.2020.167297
Received 6 October 2019; Received in revised form 2 August 2020; Accepted 3 August 2020
Available online 06 August 2020

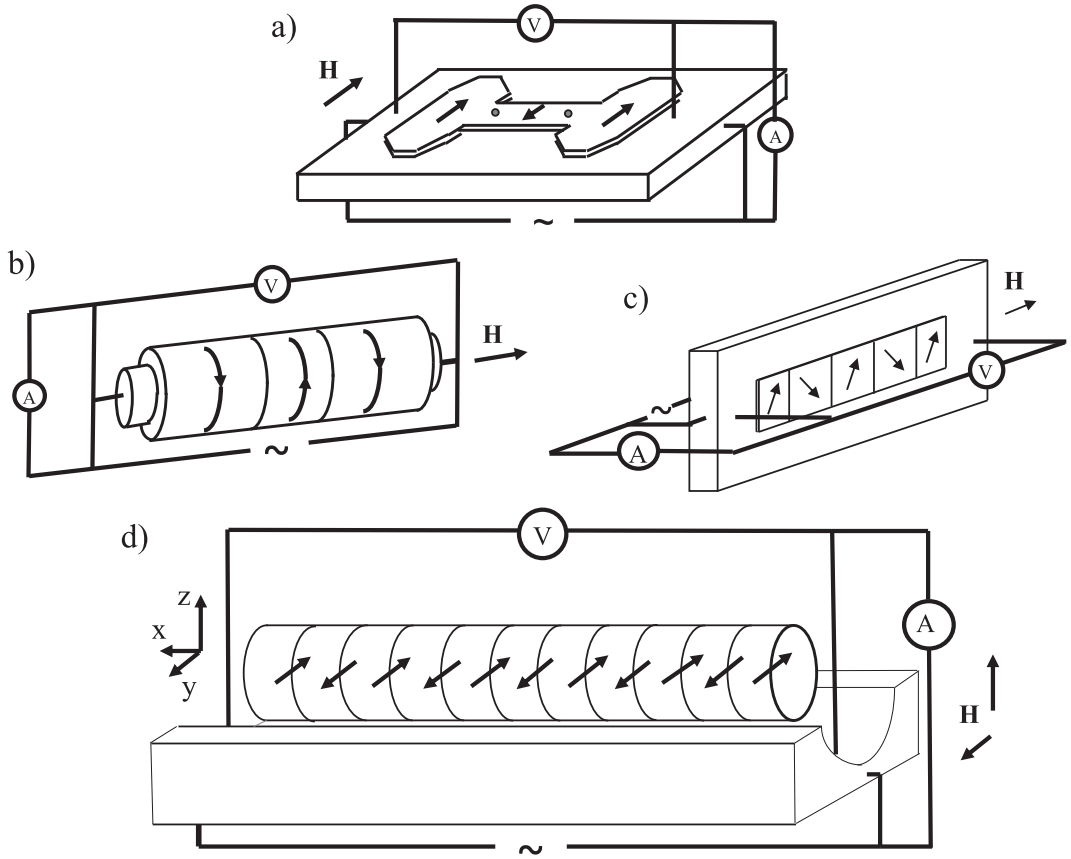

Fig. 1. Schemes of the circuits considered for GMX based on: a double vortex in H-letter-shaped nanomagnet (a), a magnetic nanotube (b), a magnetic nanostripe (c), a magnetic nanowire (d).

coherent magnetization rotation in multilayers [18–20], while, that composite mechanism of GMI is not of our interest here.

The common property of all the mentioned systems we studied previously is a small thickness of the magnetic layer (about 10 nm), which limits the magnetic flux through its cross-section, thus, the reactance value, (albeit, the relative field-induced changes of the reactance are giant) [13–15]. In the present paper, with micromagnetic simulations, we predict perpendicular GMX in a circular single-crystalline nanowire of cobalt with easy-axis transverse to the long axis, for the diameter of 50 nm, (Fig. 1d), whose area of the largest (longitudinal) cross-section (in the plane of the inductive loop) is bigger than for the magnets of our previous interest. Because of denser packing of the magnetic domains than in the systems in Fig. 1,b,c, [13,14], the amplitude of the oscillatory motion of DWs (driven by an alternating field) can be reduced without reducing the amplitude of changes of the magnetic flux through the plane.

The single-crystalline Co nanowires of the easy axis transverse to the wire axis are manufactured via electro-deposition into an anodic template [21–24]. A regular many-domain structure can be established via relaxation from an ordered state magnetized perpendicular to the easy axis and to the wire axis. In the relaxed many-domain state, DWs are magnetized in the initial direction. The resulting nonzero net magnetization is the reason of the asymmetry of the GMX effect with respect to the reversal of the perpendicular magnetic field, which is desired when sensing the field orientation (up or down of z-axis of Fig. 1d). Unlike in [13,14], where the so called longitudinal GMX has been studied, with regard to the nanowire, we focus on the "perpendicular MX" and "transverse MX", named due to the orientation of the external static field perpendicular or parallel to the easy-axis while in the plane normal to the long axis of the nanowire [25,26]. We do not study the longitudinal MX in detail because the magnetic structure is much more stiff under the action of the longitudinal field than the transverse or perpendicular ones.

In Section 2, we present a model of the single-crystalline nanowire and outline the method of evaluating MX of the system. The results of the numerical studies of the dynamical magnetic response and MX are provided in Section 3. Final conclusions are formulated in Section 4.

2. Model

2.1. Equation of motion

The single-crystalline nanowires of hcp cobalt are fabricated with the diameters of dozens of nanometers with c-axis (the easy magnetization axis) perpendicular to the wire. The magnetization of the nanowire evolves according to the Landau-Lifshitz-Gilbert (LLG) equation

$$-\frac{\partial \mathbf{M}}{\partial t} = \frac{2\gamma A_{ex}}{M_s^2}\mathbf{M}\times\Delta\mathbf{M} + \gamma\mathbf{M}\times(\mathbf{B}_{ms}+\mathbf{B}_{Oe}+\mathbf{B}) + \frac{2\gamma K_1}{M_s^2}(\mathbf{M}\cdot\hat{j})\mathbf{M}\times\hat{j} - \frac{\alpha}{M_s}\mathbf{M}\times\frac{\partial \mathbf{M}}{\partial t}. \quad (1)$$

The easy direction corresponds to the versor $\hat{j} \equiv [0, 1, 0]$ while the wire is directed along the x-axis. The saturation magnetization $M_s = |\mathbf{M}|$, A_{ex} denotes the exchange stiffness, γ – the gyromagnetic ratio, K_1 – the constant of the uniaxial (crystalline) anisotropy, α – the Gilbert damping constant. Magnetostatic and external fields are denoted by $\mathbf{B}_{ms}$ and $\mathbf{B}$, respectively. An alternating Oersted-field $\mathbf{B}_{Oe} = [0, \mu_0 H_y', 0]$ is applied in the direction of the domain magnetization, (Fig. 1d), in order to drive the oscillations of the DW positions.

Here, we restrict our considerations to the magnetic structure

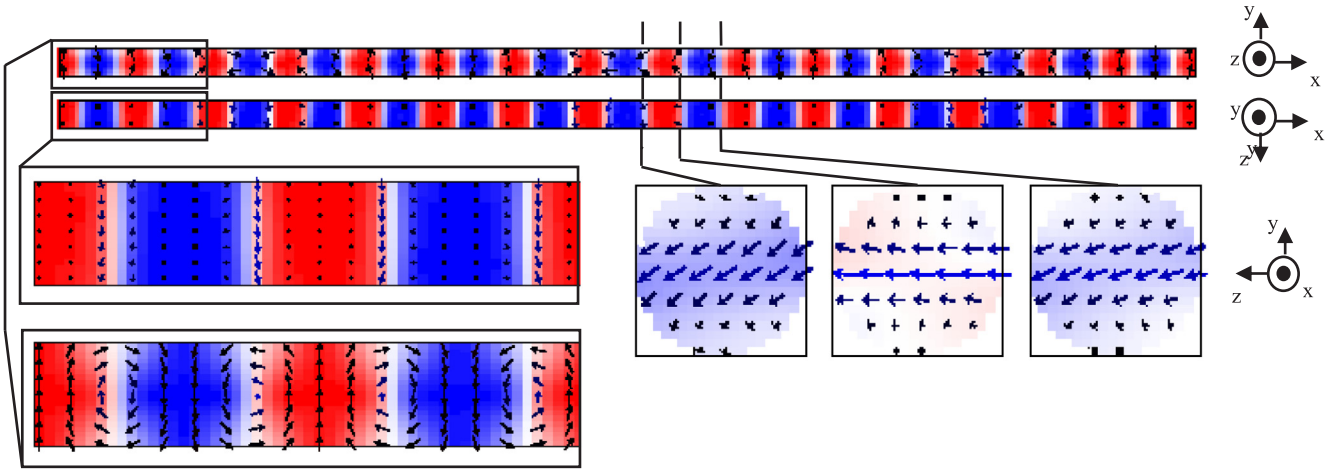

Fig. 2. The magnetization distribution in 2 μm-long, ($x \in [0, 2\,\mu m]$), and of 50-nm diameter single-crystalline Co nanowire, relaxed from the state of uniform magnetization in the z-axis direction. Here, y-axis is the easy direction. In bottom line: the magnetization in the DW areas ($x = 1.055\,\mu m$, $1.12\,\mu m$, $1.185\,\mu m$). The colors indicate the magnetization projection onto y-axis.

relaxed from a state uniformly-magnetized in the z-axis direction (the hard magnetic direction perpendicular to the nanowire axis), which results in a periodic many-domain state with Bloch DWs all magnetized parallel (with opposite chiralities to their neighbors). The observed stability of such a state of similarly magnetized DWs is quite unexpected since, according to 1D model, the equaly magnetized DWs attract each other [27]. However, in the periodic structure of densely-packed DWs, attractive binary interactions are compensated. Similar to the nanostripe edges in [14], a stabilizing role is played by the surface of the nanowire. Some deformations of DW at the surface vicinity result in an increased mutual overlap of them, (seen in the z-slice view of the magnetization in contrast to the y-slice view: the top line vs. the middle line of Fig. 2). The strong interactions allow for the driven oscillations of the magnetization to be stable, unlike e.g. the driven oscillations in thin-wall magnetic nanotubes of [13].

Let us note that the domain structure relaxed from the disordered state is known to contain circumferentially-magnetized (vortex-type) domains, however, our simulations have shown it not to be as regular as that considered here, (see also [22,28]). In the circuit with the present magnetic subsystem of the uniaxially-magnetized domains (Fig. 1d), the driving AC current does not flow trough the magnet, which is advantageous with regard to its heating. Also, the uniaxial domain ordering allows for creating the magnetic flux trough a relatively large cross-section of the ferromagnet.

In the present paper, the direction of the domain magnetization (y-axis) is called the transverse direction in contrast to z-axis direction called the perpendicular one. This nomenclature is connected to the names: transverse, perpendicular and longitudinal MI (MX) introduced in [25,26] and corresponding to the direction of the static field applied $\mathbf{B} = [0, 0, \mu_0 H_z]$ or $\mathbf{B} = [0, \mu_0 H_y, 0]$, respectively. The longitudinal MX in our nanowire is found to be a minor effect because the (anisotropy and magnetostatic) energy cost of the field-induced magnetization deviations in the xy-plane is high. The most significant is the perpendicular MX which is of our main interest, however, we study the transverse MX as well since positioning the easy axis of the nanowire in sensors can be fraught with an error.

For detailed analytical model of the dynamical response of the many-domain system to the alternating (Oersted) field, we refer to [14]. There, it has been developed with relevance to the nanostripes, based on previous considerations of the DW-induced MI in conducting magnetic ribbons in [18,19] and on the Walker model of the field-driven DW dynamics [29,30]. However, for the present system with extremely strong DW interactions, the analytical model does not allow for quantitative evaluations. We determine MX characteristics based on the simulations only. In particular, we evaluate for the ratio of the field-induced shift of the reactance to the reactance at a reference field (the so called MX ratio). Applying the AC Ohm's law, we rewrite MX ratio as a proportion of the field-induced shift of the electromotive-force (EMF) amplitude to the EMF amplitude at a reference field H_{ref}

$$\Delta Z''/Z''(H) = \frac{\mathrm{Amp}[\epsilon](H) - \mathrm{Amp}[\epsilon](H_{ref})}{\mathrm{Amp}[\epsilon](H_{ref})}, \tag{2}$$

where $H = H_z$ or $H = H_y$ depending on whether perpendicular or transverse MX is considered [31]. Here and below, $\mathrm{Amp}[\cdot]$ denotes the amplitude of any oscillating quantity. The inductive loops in the circuit of Fig. 1d is considered to be infinitely thin, thus, the EMF amplitude takes the maximum value. This makes the estimations independent of particular realization of the circuit and this allows for comparison of the results with our previous works on MX in different nanomagnets (of Fig. 1a-c). Denote y-component of the magnetization averaged over the largest cross-section of the nanowire in the plane of the inductive loop by μ_y. Thus, $\mu_y \equiv (2RLM_s)^{-1} \int_{-R}^{R} \int_{0}^{L} M_y|_{y=0}\,dx dz$), where R denotes the nanowire radius while L its length. Provided the dynamical response of the system is linear, (thus, $\mu_y(t) \propto H_y'(t)$), the magnet contribution to EMF is

$$\epsilon = -\mu_0 2RL(\dot{H}_y' + M_s\dot{\mu}_y) \approx -\mu_0 2RLM_s\dot{\mu}_y \tag{3}$$

and the MX ratio can by expressed by the amplitude of the average magnetization

$$\Delta Z''/Z''(H) \approx \frac{\mathrm{Amp}[\mu_y](H) - \mathrm{Amp}[\mu_y](H_{ref})}{\mathrm{Amp}[\mu_y](H_{ref})}. \tag{4}$$

Avoiding precise definition of shape of the conducting ingredient that generates the Oersted field, we just specify the Oersted-field amplitude while noticing its value (up to 25kA/m) to be achievable with a reasonable value of amplitude of the current density (see [13,14]).

3. Simulation results

Micromagnetic simulations of the dynamical response to the alternating transverse field have been performed for 2 μm-long and of 50 nm-diameter crystalline nanowire of cobalt with the following material parameters: $A_{ex} = 3.3{\cdot}10^{-11}$J/m, $M_s = 1.4{\cdot}10^3$ kA/m, $K_1 = 4.5{\cdot}10^5$J/m^3, $\gamma\mu_0 = 2.21{\cdot}10^5$ m/As, ($\mu_0 = 1.26{\cdot}10^{-6}$N/A^2) [32,33]. The OOMMF package (the finite-difference method, [34]) has been applied and the grid discretization size was 2.5 nm in the y- and z-directions while 5 nm in the x-direction. We arbitrarily choose the amplitude of the alternating Oersted field from the range 0÷25kA/m

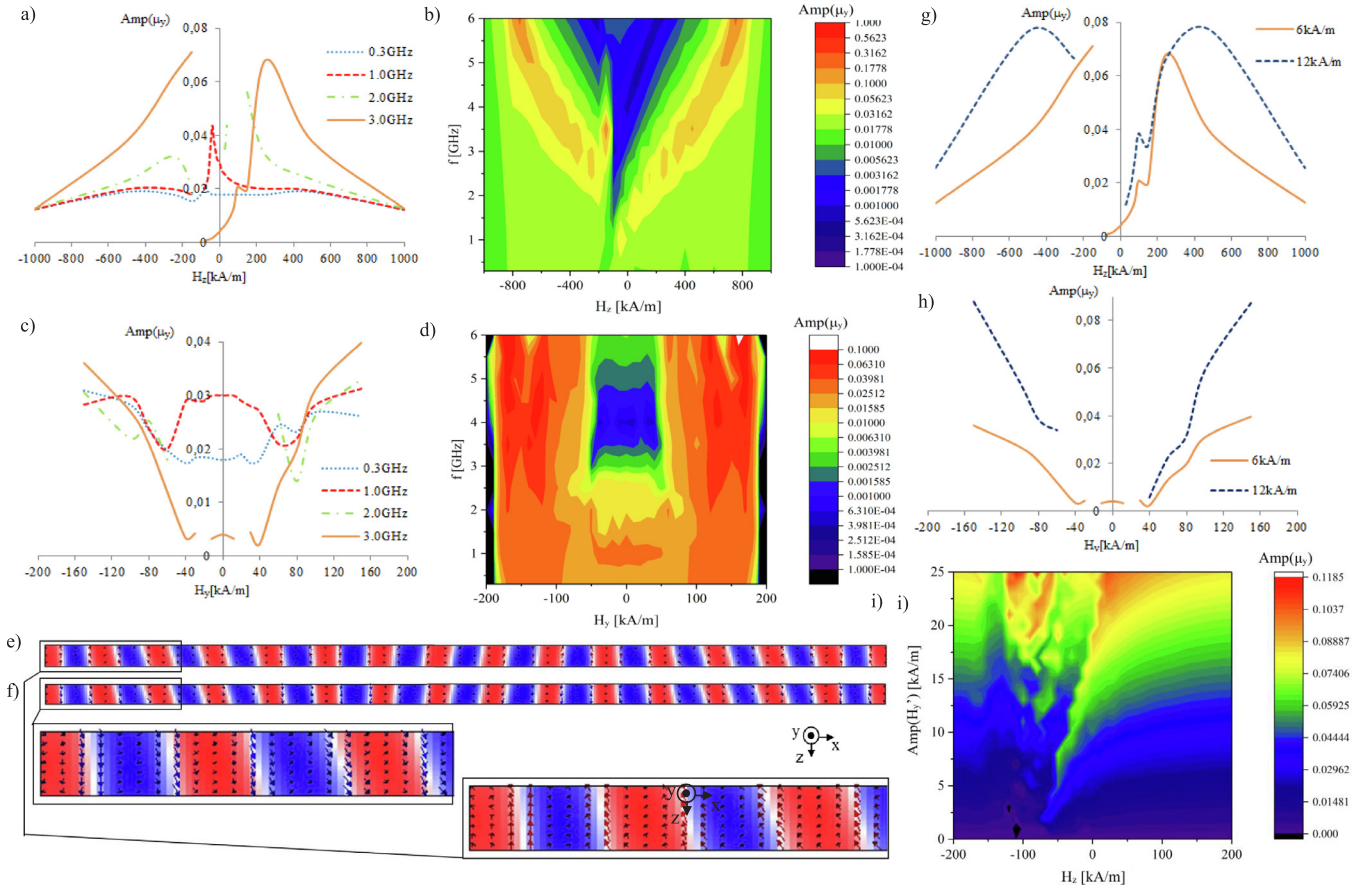

Fig. 3. The amplitude of the normalized transverse magnetization averaged over the long cross-section ($y = 0$ plane) of the nanowire with dependence on the perpendicular field H_z and AC frequency; (a), (b), and on the transverse field H_y and AC frequency; (c), (d). For (a)-(d), the amplitude of the driving (Oersted) field is $\mathrm{Amp}(H_y') = 6$ kA/m. The snapshots of the magnetization distribution in a fragment of the $y = 0$ cross-section of the nanowire correspond to the major maxima of the response amplitude $\mathrm{Amp}(\mu_y)$ at 3 GHz and $H_z = 250$ kA/m (e) and $H_z = -250$ kA/m (f), (in (e) and (f), the colors indicate magnetization projection onto y-axis, the arrow colors indicate the magnetization projection onto z-axis). The corresponding to (a)-(d) plots of $\mathrm{Amp}(\mu_y)$ at 3 GHz, for the amplitudes of the driving field $\mathrm{Amp}(H_y') = 12$ kA/m are compared to those of $\mathrm{Amp}(H_y') = 6$ kA/m in (g), (h). In (i), the static-perpendicular-field and driving-field-amplitude dependence of the amplitude of the magnetic response is plotted for the AC frequency of 1 GHz.

and its frequency from the range $0.3 \div 6.0$ GHz. The static perpendicular field H_z ranges between -1000kA/m and 1000kA/m, however, the transverse field H_y is limited by the values of $\pm$ 180 kA/m which correspond to the remagnetization of the system via shrinking the domains magnetized opposite to the field.

We have plotted the amplitude $\mathrm{Amp}(\mu_y)$ of the normalized transverse magnetization averaged over the long cross-section of the nanowire with dependence on the static perpendicular or transverse field applied, for different frequencies and amplitudes of the driving (Oersted) field (Fig. 3). In the regime of linear oscillations of the magnetization, following (4), the plots of the MX ratio are of the similar shape to the plots of $\mathrm{Amp}(\mu_y)$. It is convenient that the reference field H_{ref} in (4) was the same for the perpendicular and transverse MX, thus, let us take $H_{ref} = 0$, (whenever $\mathrm{Amp}[\mu_y](0)$ is determined). The plot lines in Fig. 3 are cut in the areas of the field where $\mathrm{Amp}(\mu_y)$ oscillates chaotically in time.

The magnetic dynamical response of the nanowire is attributed to the oscillatory motion of DWs driven by the alternating field. However, the amplitudes of oscillations of the DW positions are extremely small compared to previously studied DW systems under the Oersted field of comparable frequencies [13,14]. It is compensated by a large number of DWs. The field dependence of the response amplitude (thus, MX) is due to the field-induced deviation of the domain magnetization and/or the field-induced change of the DW width. While the transverse MX is almost symmetric with respect to the inversion of the field ($H_y \to -H_y$, Fig. 3c,d,h), perpendicular MX is clearly asymmetric (with respect to the change $H_z \to -H_z$, Fig. 3a,b,g). The asymmetry is related to the fact that all DWs are magnetized into + z-direction, hence, the H_z-field influences the widths of all DWs in the same manner.

A specific feature of the plots of $\mathrm{Amp}[\mu_y](H_z)$ is a dependence of the position of a sharp local maximum (in the low-field area) on the AC frequency. From Fig. 3a, comparing the dashed red line of 1 GHz curve to the continuous beige line of 3 GHz curve, one sees a local maximum to correspond to a negative field in the former curve while to a positive field in the later one. Thus, the curve slope changes between the negative and positive ones at zero field. However, in snapshots taken during the time evolution of the system, we have not seen differences in the magnetic structure under the 1 GHz and 3 GHz driving (in the domain nor DW areas). Two competing effects: the field-induced change of the DW width and the frequency dependence of the amplitude of the driven DW motion allow for the explanation of that plot peculiarity. The DW width increases with the positive H_z field, which leads to the increase of the DW velocity and, hence, the amplitude of oscillations of the DW center. On the other hand, this amplitude increases with the oscillation period. Since the motion amplitude is limited by strong interactions between DWs, in the case of a sufficiently-large period, the decrease of the DW width under the negative H_z field is advantageous leading to a reduction of the overlap of the interacting DWs. Our view is supported by the plot of the response amplitude with dependence on the perpendicular field and the driving-field amplitude

for the frequency of 1 GHz (Fig. 3i). In the plot, one sees a shift of the maximum of $\mathrm{Amp}[\mu_y](H_z)$ with increase of the amplitude of the driving field towards higher values of H_z, which is related to the increase of the DW-motion amplitude.

The major maxima of the dynamical response of the system are located symmetrically on both sides of the vertical axis in $\mathrm{Amp}[\mu_y](H_z)$ plots (Fig. 3a,b,g), in the areas $|H_z|$~200 ÷ 500 kA/m. Unlike the corresponding plots in Refs. [13,14] (devoted to the systems in Fig. 1b,c), these maxima are not directly related to the thin-film FMR. The domain structure remains stable during the evolution for the whole range of the field H_z of the plots. The specific behavior of the system in the vicinity of the maxima of H_z are high-amplitude rotational oscillations of orientation of the DW normal in the xz-plane (Fig. 3e,f). They are accompanied by oscillations of the DW widths, (the so called DW bulging [35,36]), strongly influencing the dynamical magnetic response. Also, it is seen with arrows in Fig. 3e,f that the DW magnetization is parallel or antiparallel to z-axis depending on the sign of H_z. It is so in the high-field area of the dynamical response $|H_z| > 150$ kA/m, and the DW remagnetization explains the symmetry of the plots in Fig. 3,a,b,g, in the high-field regime.

4. Conclusions

We have studied the dynamical response of the single-crystalline Co nanowire with relevance to MX. Perpendicular MX is found to be asymmetric in the field range $H_z \in (-100, 100)$ kA/m. Calculating the MX ratio with (4), for $H_{ref} = 0$, we have established perpendicular MX to achieve $\Delta Z''/Z''$ (250 kA/m) = 1400% at the AC frequency of 3 GHz and the driving-field amplitude $\mathrm{Amp}(H_y') = 6$ kA/m (the solid line in Fig. 3a and g), in the low-field range of the monotonic $\Delta Z''/Z''(H_z)$ dependence; $\Delta Z''/Z''$ (100 kA/m) = 400%. These large values are achievable due to the stability of the magnetic structure in a wide range of the field which is related to the magnetic hardness of the cobalt nanowire. The domain structure is conserved in the range of the perpendicular field $H_z \in [-1000$ kA/m, 1000 kA/m] (however, for $H_z < -150$ kA/m, DW magnetization is reversed). Also, the structure is stable in a relatively wide range of the transverse field $|H_y| < 180$ kA/m, (up to the domain-remagnetization field). This is an advantage compared to the systems of [13,14], (Fig. 1b,c), whose high-field longitudinal MX is related to the thin-film FMR. Since FMR breaks the domain structure and may cause the relaxation to different magnetization states, its absence is propitious for the sensor durability.

At the frequency of 3 GHz, the sensitivity of perpendicular MX; $d(\Delta Z''/Z)/dH_z$ (relevant to the solid line in Fig. 3a,g) takes 2.4%· m/kA at $H_z = 0$, while, at $H_z = 90$ kA/m, it takes 9%· m/kA. These values of the field sensitivity are comparable to ones predicted for nanotubes and nanostripes of [13,14], while, considerably smaller than obtainable with the soft-ferromagnetic system of [15] which is operated in a narrower range of the field. However, good MX characteristics of the later system have been found under conditions of a resonance in the double-vortex system, which is not desirable with regard to the sensor reliability. It should be noticed that the highlighted GMX characteristics of the Co nanowire are achievable with very small amplitude of the DW movement. Unlike in the systems of DWs densely packed in the nanostripes of [14], for the frequency range of our study, we avoid resonant increase of the DW-oscillation amplitude. The small amplitude limits the dynamical magnetic response which is compensated, however, by a very high density of the DWs and a relatively large area of the nanowire cross-section (in the plane of the inductive loop) that generates the time-dependent magnetic flux.

CRediT authorship contribution statement

Andrzej Janutka: Conceptualization, Investigation, Supervision, Writing - original draft. **Kacper Brzuszek:** Investigation, Visualization.

Declaration of Competing Interest

The authors declare that they have no known competing financial interests or personal relationships that could have appeared to influence the work reported in this paper.

Acknowledgement

Calculations have been carried out using resources provided by Wroclaw Centre for Networking and Supercomputing (http://wcss.pl), Grant No. 450.

References

[1] M. Knobel, M. Vazquez, L. Kraus, Giant Magnetoimpedance, in: K.H.J. Buschow (Eds.), Handbook of Magnetic Materials, vol. 15, pp. 497–563 (Elsevier 2003).
[2] M.-H. Phan, H.-X. Peng, Giant magnetoimpedance materials: Fundamentals and applications, Prog. Mater. Sci. 53 (2008) 323.
[3] A. Zhukov, M. Ipatov, V. Zhukova, Advances in Giant Magnetoimpedance of Materials, in: K.H.J. Buschow (Eds.), Handbook of Magnetic Materials, vol. 24, pp. 139–236 (Elsevier 2015).
[4] A. Garcia-Arribas, E. Fernandez, D. de Cos, Thin-Film Magneto-Impedance Sensors, in: A. Asfour (Eds.) Magnetic Sensors: Development Trends and Applications, pp. 39–62 (IntechOpen 2017).
[5] K.S. Nakayama, T. Chiba, S. Tsukimoto, Y. Yokoyama, T. Shima, S. Yabukami, Ferromagnetic resonance in soft-magnetic metallic glass nanowire and microwire, Appl. Phys. Lett. 105 (2014) 202403.
[6] G.V. Kurlyandskaya, A.V. Svalov, E. Fernandez, A. Garcia-Arribas, J.M. Barandiaran, FeNi-based magnetic layered nanostructures: magnetic properties and giant magnetoimpedance, J. Appl. Phys. 107 (2010) 09C502.
[7] H. Chiriac, O.-G. Dragos, M. Grigoras, G. Ababei, N. Lupu, Magnetotransport phenomena in [NiFe/Cu] magnetic multilayered nanowires, IEEE Trans. Magn. 45 (2009) 4077.
[8] F.E. Atalay, H. Kaya, S. Atalay, E. Aydogmus, Magnetoimpedance effects in a CoNiFe nanowire array, J. Alloys Comp. 561 (2013) 71.
[9] J. Devkota, A. Ruiz, P. Mukherjee, H. Srikanth, M.H. Phan, A. Zhukov, V.S. Larin, Magneto-resistance, magneto-reactance, and magneto-impedance effects in single and multi-wire systems, J. Alloys Compd. 549 (2013) 295.
[10] J. Devkota, C. Wang, A. Ruiz, S. Mohapatra, P. Mukherjee, H. Srikanth, M.H. Phan, Detection of low-concentration superparamagnetic nanoparticles using an integrated radio frequency magnetic biosensor, J. Appl. Phys. 113 (2013) 104701.
[11] J. Devkota, M. Howell, P. Mukherjee, H. Srikanth, S. Mohapatra, M.H. Phan, Magneto-reactance based detection of MnO nanoparticle-embedded Lewis lung carcinoma cells, J. Appl. Phys. 117 (2015) 17D123.
[12] Tao Wang, et al., Detection of a rectangular crack in martensitic stainless steel using a magnetoreactance sensing system, IEEE Magn. Lett. 9 (2018) 6502404.
[13] A. Janutka, K. Brzuszek, Domain-wall-assisted giant magnetoimpedance of thin-wall ferromagnetic nanotubes, J. Magn. Magn. Mater. 465 (2018) 437.
[14] A. Janutka, K. Brzuszek, Domain-wall-assisted asymmetric magnetoimpedance in ferromagnetic nanostripes, J. Phys. D: Appl. Phys. 52 (2019) 035003.
[15] A. Janutka, K. Brzuszek, Double-vortex-assisted asymmetric magnetoreactance in H-shaped nanomagnets, IEEE Magn. Lett. 10 (2019) 6103105.
[16] R. Valenzuela, Low-frequency magnetoimpedance: domain wall magnetization processes, Physica B 299 (2001) 280.
[17] P. Ciureanu, L.G.C. Melo, D. Seddaoui, D. Menard, A. Yelon, Physical models of magnetoimpedance, J. Appl. Phys. 102 (2007) 073908.
[18] F.L.A. Machado, S.M. Rezende, A theoretical model for the giant magnetoimpedance in ribbons of amorphous soft-ferromagnetic alloys, J. Appl. Phys. 79 (1996) 6558.
[19] D. Atkinson, S.T. Squire, Phenonemological model for magnetoimpedance in soft ferromagnets, J. Appl. Phys. 83 (1998) 6569.
[20] G.V. Kurlyandskaya, L. Elbaile, F. Alves, B. Ahamada, R. Barrue, A.V. Svalov, V.O. Vas'kovskiy, Domain structure and magnetization process of a giant magnetoimpedance geometry FeNi/Cu/FeNi(Cu)FeNi/Cu/FeNi sensitive element, J. Phys.: Cond. 16 (2004) 6561.
[21] Yu.P. Ivanov, D.G. Trabada, A. Chuvilin, J. Kosel, O. Chubykalo-Fesenko, M. Vazquez, Crystallographically driven magnetic behaviour of arrays of monocrystalline Co nanowires, Nanotechnology 25 (2014) 475702.
[22] Yu.P. Ivanov, A. Chuvilin, L.G. Vivas, J. Kosel, O. Chubykalo-Fesenko, M. Vazquez, Single crystalline cylindrical nanowires – toward dense 3D arrays of magnetic vortices, Sci. Rep. 6 (2016) 23844.
[23] M. Stano, O. Fruchart, Magnetic nanowires and nanotubes, in: E. Bruck (Eds.), Handbook of Magnetic Materials, vol. 27, pp. 155–268 (Elsevier 2018).
[24] J. Alam, et al., Cylindrical micro and nanowires: fabrication, properties and applications, J. Magn. Magn. Mater. 513 (2020) 167074.
[25] R.L. Sommer, C.L. Chien, Longitudinal and transverse magneto-impedance in amorphous Fe73.5Cu1Nb3Si13.5B9 films, Appl. Phys. Lett. 67 (1995) 3346.
[26] R.L. Sommer, C.L. Chien, Longitudinal, transverse, and perpendicular magnetoimpedance in nearly zero magnetostrictive amorphous alloys, Phys. Rev. B 53 (1996) R5982.
[27] A. Janutka, Complexes of domain walls in one-dimensional ferromagnets near and

far from phase transition, Acta Phys. Pol. A 124 (2013) 23.
[28] J.A. Fernandez-Roldan, D. Chrischon, L.S. Dorneles, O. Chubykalo-Fesenko, M. Vazquez, C. Bran, A comparative study of magnetic properties of large diameter Co nanowires and nanotubes, Nanomaterials 8 (2018) 692.
[29] N.L. Schryer, L.R. Walker, The motion of 180° domain walls in uniform dc magnetic fields, J. Appl. Phys. 45 (1974) 5406.
[30] G.S.D. Beach, C. Knutson, M. Tsoi, J.L. Erskine, Field- and current-driven domain wall dynamics: an experimental picture, J. Magn. Magn. Mater. 310 (2007) 2038.
[31] M. Velazquez, M. Vazquez, D.-X. Chen, A. Hernando, Giant magnetoimpedance in nonmagnetostrictive amorphous wire, Phys. Rev. B 50 (1994) 16737.
[32] H. Kronmuller, M. Fahnle, Micromagnetism and the Microsructure of Ferromagnetic Solids, Cambridge University Press, 2003.
[33] R. Moreno, R.F.L. Evans, Temperature-dependent exchange stiffness and domain wall width in Co, Phys. Rev. B 94 (2016) 104433.
[34] http://math.nist.gov/oommf/.
[35] K.L. Garcia, R. Valenzuela, Domain wall pinning, bulging, and displacement in circumferential domains in CoFeBSi amorphous wire, J. Appl. Phys. 87 (2000) 5257.
[36] R. Valenzuela, The analysis of magnetoimpedance by equivalent circuits, J. Magn. Magn. Mat. 249 (2002) 300.